applied sciences

MDPI

Article

Study on the Rheological Performance and Microscopic Mechanism of PPA/SBS/SBR Composite-Modified Asphalt Cold Replenishment Liquid

Zongjie Yu [1,2,*], Xiaoyi Ban [3], Yafeng Xu [1,2], Xiaosong Liu [3], Lei Ma [1,2], Shujun Liu [1,2], Zengping Zhang [3,*] and Yueming Zhou [1,2]

[1] Xinjiang Institute of Transportation Sciences Co., Ltd., Urumqi 830000, China; yafx1970@163.com (Y.X.); leim1991@163.com (L.M.); shunjl1976@163.com (S.L.); zhouyueming6929@163.com (Y.Z.)
[2] Key Laboratory of Highway Engineering Technology and Transportation Industry in Arid Desert Regions, Urumqi 830000, China
[3] Key Laboratory for Special Area Highway Engineering of Ministry of Education, Chang'an University, Xi'an 710064, China; 2021021087@chd.edu.cn (X.B.); 2021221259@chd.edu.cn (X.L.)
* Correspondence: 13511844380@163.com (Z.Y.); glping@chd.edu.cn (Z.Z.)

Abstract: To prepare high-performance asphalt cold replacement liquids, a composite modification preparation process was used to synthesize a styrene–butadiene–styrene (SBS) block copolymer, styrene–butadiene–rubber (SBR) copolymer, and polyphosphate acid (PPA), erucamide/diesel/acrylic ester as surfactants/diluents/reinforcing agent respectively. These six were blended to prepare an asphalt cold replenishment liquid (ACRL), and its modification effect on base asphalt was studied using base asphalt as the control group. A comparative study was conducted on the high- and low-temperature rheological properties and microstructure. The modification mechanisms of high-temperature asphalt cold replenishment liquid (H-ACRL) and low-temperature asphalt cold replenishment liquid (L-ACRL) were studied through dynamic shear rheometry, bending beam rheometry, Fourier-transform infrared spectroscopy, fluorescence microscopy, and atomic force microscopy. The results showed that the optimal dosages of PPA/SBS/SBR in H-ACRL and L-ACRL were (1.2%/5%/3%) and (0.9%/4%/4%), respectively. Within the optimal dosage range, the particles in the cold replenishment fluid were uniformly dispersed in the asphalt to form a dense and continuous network. No new functional groups were generated during the preparation of H-ACRL and L-ACRL, showing that the modifiers (surfactants/diluents/reinforcing agent) were only physically blended with the asphalt.

Keywords: PPA/SBS/SBR composite; composite modification; asphalt cold replacement fluid; modification mechanism; rheological properties

check for updates

Citation: Yu, Z.; Ban, X.; Xu, Y.; Liu, X.; Ma, L.; Liu, S.; Zhang, Z.; Zhou, Y. Study on the Rheological Performance and Microscopic Mechanism of PPA/SBS/SBR Composite-Modified Asphalt Cold Replenishment Liquid. *Appl. Sci.* **2023**, *13*, 11193. https://doi.org/10.3390/app132011193

Academic Editor: Ana Martins Amaro

Received: 16 September 2023
Revised: 7 October 2023
Accepted: 9 October 2023
Published: 11 October 2023

Copyright: © 2023 by the authors. Licensee MDPI, Basel, Switzerland. This article is an open access article distributed under the terms and conditions of the Creative Commons Attribution (CC BY) license (https://creativecommons.org/licenses/by/4.0/).

1. Introduction

Asphalt pavement has a flat surface, no joints, driving comfortability, low noise, a short construction period, and simple maintenance, but due to long-term traffic loads, low temperatures, and water, it is easily damaged [1], causing it to gradually become loose and produce pits and grooves that impede traffic. During the initial stage of damage, these defects generally lead to small-scale damage, but if they are not treated quickly or effectively, the area and depth of pits and grooves will spread, causing secondary damage to the pavement or even large-scale damage. This will reduce the service life of pavement, affect driving comfort, and even cause traffic accidents [2,3]. Due to gradual improvements in China's highway network, most pavement defects are repaired instead of reconstructed. Therefore, the selection of the pit repair method for asphalt pavement is important.

Hot-mix asphalt (HMA) is generally used to repair pavement pits whose high- and low-temperature performance and water stability are excellent. However, specific equipment is

required during mixing, and a higher temperature is required during mixing and paving construction. When repair works are scattered and the defective area is small, the hot repair method is not economical and is greatly affected by environmental factors. This makes it unsuitable for construction in harsh environments such as low temperatures, rain, and snow [4,5].

The cold patching method seals and stores a pre-prepared cold patching asphalt mixture (CPAM) in a bag, which can be used at ambient temperatures for all-weather pit repair. However, compared with HMA, the adhesion performance of CPAM is worse due to the sharp decline in the adhesion of the asphalt binder with a diluent. Under traffic loads and water damage, it shows low early strength, weak bearing capacity, and poor water stability, resulting in looseness, peeling, and other short-term defects [6,7]. Compared with HMA, CPAM can be used in poor weather conditions, such as rain and snow, and is less affected by the external environment. It also has the advantages of simple construction and energy conservation.

However, the performance of CPAM mainly depends on the performance index of modified asphalt. In addition, researchers are committed to researching CPAM composite-modified asphalt additives to improve the performance of CPAM [8–12]. For example, waterborne acrylate and polyurethane can improve the storage stability and high-temperature performance of SBS/SBR-modified asphalt. Adding various polymers and composite modifiers can also improve the high and low-temperature performance, water stability, and adhesion of CPAM. However, due to the different density, polarity, and molecular structure between polymers and asphalt, their compatibility is poor, and they easily separate when stored at high temperatures.

In recent years, studies have shown that polyhydroxyalkanoites (PHAs), MoS2 quantum dots (MQDs), zinc sulfide (ZnS), and nanoparticles (NPs) are beneficial for improving the thermal stability and tensile strength of composite materials [13–15]. In contrast, the research on PPA modifiers has achieved significant results and applications. One study found that PPA-modified asphalt showed better high-temperature performance and storage stability than asphalt, but its low-temperature performance was poor. The use of synthesized styrene–butadiene–styrene (SBS) block copolymer and styrene–butadiene–rubber (SBR) co-polymer significantly improved the high-temperature performance of the asphalt. Therefore, the use of a PPA/SBS/SBR composite-modified asphalt may change the asphalt's performance. Existing research has investigated the high-temperature performance, low-temperature performance, and modification mechanism of PPA/SBR composite-modified asphalt and asphalt mixtures. However, research on the high-temperature and low-temperature performance and anti-aging ability of PPA/SBS/SBR composite-modified asphalt is relatively rare [16,17].

This article adopted a composite modification preparation process using PPA/SBS/SBR to prepare high-temperature asphalt cold replenishment liquid (H-ACRL) and low-temperature asphalt cold replenishment liquid (L-ACRL) and studied their modification effects on base asphalt. First, the influence of additives such as PPA/SBS/SBR, erucamide, diesel, and acrylic ester on the performance of H-ACRL and L-ACRL was studied through routine physical performance tests. The optimal dosage of PPA/SBS/SBR modifiers and erucamide/diesel/acrylic ester additives was determined. Secondly, the performance and modification mechanism of H-ACRL and L-ACRL were evaluated through dynamic shear rheology (DSR), bending beam rheometry (BBR), fluorescence microscopy, Fourier-transform infrared (FTIR) spectroscopy, and atomic force microscopy, and compared to those of base asphalt. These results provide an experimental basis for promoting the applications of asphalt cold replenishment liquid (ACRL) technology.

2. Experimental Materials and Methods

2.1. Materials

Polyphosphoric acid (PPA), styrene–butadiene–styrene (SBS) block copolymer, and styrene–butadiene–rubber (SBR) copolymer were selected as modifiers for Karamay 90#

asphalt from Karamay Petrochemical Co., Ltd, Xinjiang, China. The morphologies of the three modifier samples are shown in Figure 1.



(**a**) SBR modifier (**b**) SBS modifier (**c**) PPA modifier

Figure 1. Sample morphology of modifier.

2.1.1. 90# Base Asphalt

A 90# asphalt from PetroChina Karamay Petrochemical Co., Ltd, Xinjiang, China. was selected as the base asphalt, and the main performance index test results are shown in Table 1.

Table 1. Main performance indexes of base asphalt.

Performance Index		Detection Result
Penetration (25 °C) (0.1 mm)		82
Penetration index PI		−0.95
Softening point (°C)		45.5
Dynamic viscosity at 60 °C (Pa·s)		269
Ductility (15 °C)cm		>100
Ductility (10 °C)cm		>100
Solubility (%)		99.79
Wax content (%)		1.8
Flash point (°C)		296
Residue after TFOT	Quality change (%)	−0.091
	Residual penetration ratio (25 °C) (0.1 mm)	61.7
	Residual ductility (5 °C) cm	29

2.1.2. Polyphosphoric Acid

Polyphosphate is a mixture of phosphoric acids (ortho, pyro, tri, and tetra) with a content of over 68% phosphoric anhydride, which has a certain degree of corrosiveness. It is a colorless, transparent, viscous liquid, easily deliquescent, non-crystalline, and hard-glassy [18,19]. The PPA was produced by Xiangyang Gaolong Phosphorus Chemical Co., Ltd., with a molecular formula of $H_{n+2}P_nO_{3n+1}$. Table 2 lists its technical indicators, and Figure 2 shows the molecular structure of PPA.

Table 2. Basic characteristics of polyphosphoric acid.

Performance Index	Detection Result
Appearance	colorless liquid
Boiling point (°C)	550
Density/relative density (25 °C)	2.05 g/mL
Content (P_2O_5) (%), ≥	85

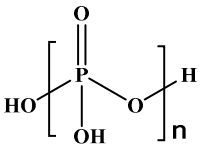


Figure 2. Molecular structure of PPA.

2.1.3. SBS and SBR

SBS particles produced by Jilin Chemical Industry Co., Ltd, Jilin, China. and SBR particles produced by Shandong Xianyuan Chemical Technology Co., Ltd., Shandong, China. were selected as the modifiers. Tables 3 and 4 list the technical indicators of SBS and SBR.

Table 3. SBS general indicators.

Performance Index	Detection Result
Appearance	White particles
Block ratio	30/70
Density (g/mL)	1.04
Tensile strength (MPa) ≥	18
300% Constant extension stress (MPa)	2.0
Shore hardness	75
Ultimate elongation (%)	815

Table 4. SBR general indicators.

Performance Index	Detection Result
Appearance	White particles
Density (g/mL)	1.04
Bound styrene (%)	22.5~24.5
Organic acid (%)	4.50~6.75
Moisture content (%) ≤	2.5
Mooney viscosity of raw rubber, 50 mL (1 + 4) 100 °C ≤	75

2.2. Preparation of PPA/SBS/SBR Composite-Modified Asphalt

Base asphalt (700 g) was heated in an oven to 130–140 °C to soften it and then placed on a shearing device. SBS and SBR were added in proportion to the base asphalt. A high-speed shearing machine (2000 r/min) was used for shearing and swelling at 140–150 °C for 50 min, and sheared at a high speed (4500 r/min) at 170–180 °C for 50 min (surfactants were added after 25 min of shearing, and stabilizers were added after 45 min). The mixture was sheared for 50 min and cooled to 145–155 °C. After 40 min of shearing at 3000 r/min, the sample was cooled to 95–105 °C and then sheared at 2000 r/min for 30 min (diluent was added after 10 min, and enhancer was added at 20 min). Finally, PPA/SBS/SBR composite-modified asphalt was prepared, and the preparation process flowchart is shown in Figure 3.

2.3. Experimental Instruments and Methods

2.3.1. Conventional Physical Indicators

According to the requirements in the "Test Specification for Asphalt and Asphalt Mixtures in Highway Engineering" (JTG E20-2011) [20], the penetration, softening point, and ductility indicators of base asphalt, H-ACRL, and L-ACRL were tested.

2.3.2. Rheological Properties

(1) Dynamic shear rheology

The DSR (model CV0150 AR1500ex) was manufactured by TA Instruments Operating Software (Austin, TX, USA). The DSR test was used to accurately evaluate the viscoelastic

properties of the asphalt. By testing the relationship between applied stress and measured strain, the composite shear modulus (G*), phase angle (δ), and rutting factor (G*/sinδ) were obtained. The test temperature range was 58–82 °C, and the heating rate was 2 °C/min.

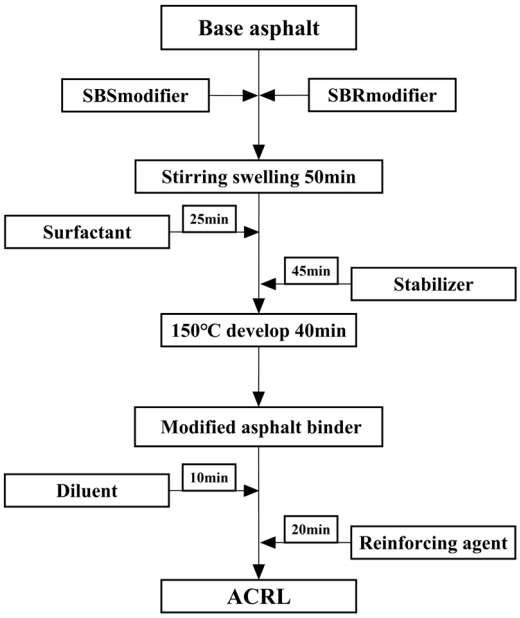


Figure 3. Process flow diagram of ACRL preparation.

(2) Bending beam rheometry

The bending beam rheometer (BBR; model PE-BBR-F) was manufactured by Cannon Corporation (Melville, NY, USA). The BBR test was used to accurately evaluate the cracking resistance of asphalt at low temperatures. By applying a constant load and measuring the deflection, the creep stiffness modulus (S) and creep rate (m) of the asphalt binder were calculated at the 60th second to evaluate the low-temperature performance of the asphalt. BBR tests were conducted on base asphalt, H-ACRL, and L-ACRL using temperatures of −30 °C, −36 °C, and −40 °C and a loading time of 240 s.

2.3.3. Thin-Film Oven Test

The short-term thermal oxygen aging of asphalt was evaluated using a thin-film oven test (TFOT) using a rotating thin-film oven manufactured by Zhejiang Chenxin Mechanical Equipment Co., Ltd., Zhejiang, China. (model SBX-82). According to the requirements in the "Test Specification for Asphalt and Asphalt Mixtures in Highway Engineering" (JTG E20-2011) [20], the base asphalt, H-ACRL, and L-ACRL were placed on an aging plate at 163 °C and tested for 5 h. The quality changes, residual penetration ratio at 25 °C, and residual ductility at 10 °C were detected after TFOT.

2.3.4. Micro-Mechanism

(1) Fluorescence microscopy

An LW300LFT fluorescence microscope was used to observe the dispersion of asphalt and additive phases in different ACRLs at a magnification ratio of 400×.

(2) Fourier-transform infrared (FTIR) spectroscopy

FTIR was performed using a Vertex70 infrared spectrometer produced by Bruker Company in Germany, with a scanning frequency of 32 times/min. FTIR spectroscopy was conducted on a PPA/SBS/SBR composite-modified asphalt with a resolution of 4 cm^{-1} and a scanning range of 400–4000 cm^{-1}.

(3) Atomic force microscopy

A Dimension Icon atomic force microscope (AFM) produced by Bruker Company in Germany was used to analyze differences in the surface morphology of PPA/SBS/SBR composite-modified asphalt and base asphalt using three-dimensional stereograms. The scanning area was 15 μm × 15 μm, the scanning rate was 1 Hz, and the resonant frequency was 260 kHz.

2.4. Vacuum Treatment Test of Asphalt Cold Replenishment Solution

A DZF-6050 vacuum drying oven produced by Shanghai Qixin Scientific Instrument Co., Ltd, Shanghai, China. was used for the ACRL vacuum drying treatment. The vacuum treatment test is to accelerate the volatilization of the diluent, and the vacuum temperature is consistent with the curing temperature of CMA. The curing conditions follow the standard [21] "JT/T 972-2015 Asphalt Pavement Pit Cold Repair Finished Material". ACRL samples were placed in the vacuum drying oven for 14 h under conditions in which the vacuum gauge value reached 0.1 MPa and the temperature was 110 °C. Experimental studies were conducted based on ACRL treated with vacuum drying.

3. Results and Discussion

3.1. Determination of the Type of PPA/SBS/SBR Composite-Modified Asphalt Cold Replenishment Liquid

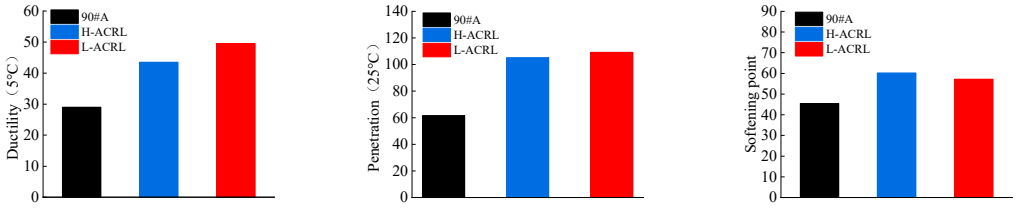
Based on previous research, PPA/SBS/SBR was used as the modifier, and erucamide/diesel/acrylic ester as surfactants/diluents/reinforcing agent respectively. An orthogonal experiment with a combination of 6 factors and 5 levels was conducted. A total of 25 sets of experiments were conducted, and the orthogonal experiments were processed through factor level and range analysis. Two different types of PPA/SBS/SBR composite-modified asphalt cold replenishment fluids were developed, whose composition ratios are shown in Table 5.

Table 5. Composition ratios of different asphalt cold replenishment fluids.

Asphalt Cold Rehydration Fluid Type	Composition Dosage (%)					
	SBS	SBR	Erucamide	Polyphosphate	Diesel Oil	Acrylate
L-ACRL	4	4	1.5	0.9	18	7
H-ACRL	5	3	0.9	1.2	15	5

3.2. Basic Indicators of PPA/SBS/SBR Composite-Modified Asphalt Cold Rehydration Solution

To conveniently record and analyze the fundamental indicators of PPA/SBS/SBR composite modified asphalt, this article refers to the high-temperature type PPA/SBS/SBR composite modified asphalt cold replenishment liquid as high-temperature type asphalt cold replenishment liquid (H-ACRL), the low-temperature type PPA/SBS/SBR composite modified asphalt cold replenishment liquid as low-temperature type asphalt cold replenishment liquid (L-ACRL), and the asphalt cold replenishment liquid as (ACRL). The basic indicators of base asphalt and different ACRLs after short-term aging are shown in Figure 4. After adding modifiers, surfactants, diluents, and reinforcing agent to the base asphalt, the penetration of PPA/SB/SB-modified asphalt increased compared to that of the base asphalt; the softening point increased; and the ductility at 5 °C increased. After adding modifiers, surfactants, diluents, and reinforcing agent, the increase in asphalt penetration was greater than 70%, mainly due to the improved flow properties of PPA/SB/SB-modified asphalt. The addition of modifiers, surfactants, diluents, and reinforcing agent to the base asphalt increased the softening point by more than 25%, indicating that modifiers, surfactants, diluents, and reinforcing agent also improved the high-temperature performance of the asphalt. The modifiers, surfactants, diluents, and reinforcing agent caused the 5 °C ductility of the asphalt to exceed 50%, indicating that modifiers, surfactants, diluents, and reinforcing agent improved the low-temperature performance of the asphalt.



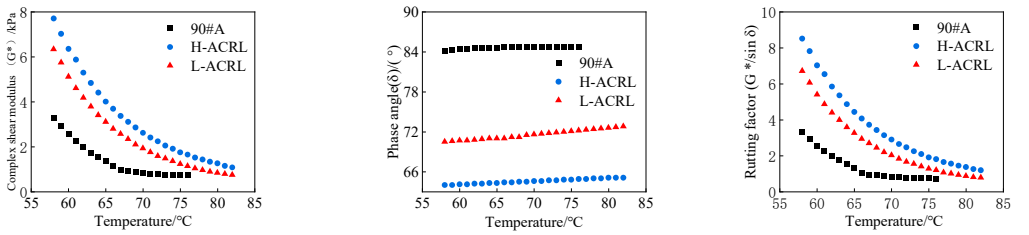
(**a**) Ductility (**b**) Penetration (**c**) Softening point

Figure 4. Three major indicators after TFOT.

3.3. Rheological Properties of PPA/SBS/SBR Composite-Modified Asphalt Cold Replacement Solution

3.3.1. High-Temperature Rheological Properties

The complex shear modulus (G*) and phase angle (δ) were obtained through DSR to reflect the viscoelastic properties of the asphalt. A higher G* value indicates better deformation resistance of the asphalt at high temperatures [22]. δ indicates changes in the viscous and elastic parts of the asphalt materials. Because asphalt is an elastoplastic, a higher δ value indicates it is more viscous and less elastic. The rutting factor (G*/sinδ) is used to evaluate the high-temperature rutting resistance of asphalt, where a larger value indicates greater high-temperature rutting resistance [23]. Temperature scanning tests were conducted on H-ACRL, L-ACRL, and base asphalt using DSR. The modifiers, surfactants, diluents, and reinforcing agent content were different in H-ACRL and L-ACRL. The results of different asphalt temperature scanning tests are shown in Figure 5.



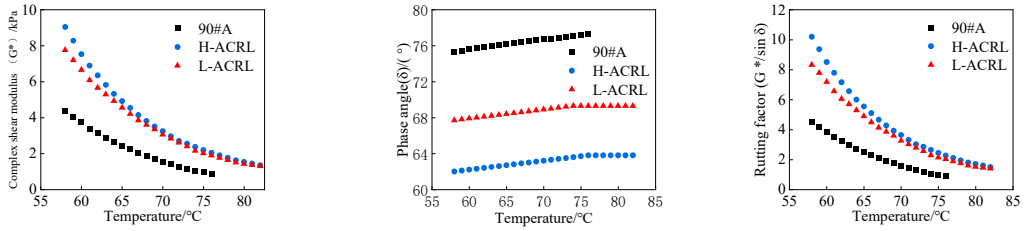
(**a**) Complex shear modulus (G*)/kPa (**b**) Phase angle (δ)/ (°) (**c**) Rutting factor (G*/sinδ)

Figure 5. Temperature scanning test results before TFOT.

Figure 5a and c show the G* values and G*/sinδ of the three types of asphalt (δ), all of which sharply decreased upon increasing the temperature, and then plateaued. This was because the asphalt gradually transitioned from a highly-elastic state to a viscous flow state upon increasing the temperature, resulting in a decrease in its deformation resistance. The G* and G*/sinδ values of the two ACRLs at the same temperature were significantly higher than those of the base asphalt, indicating that the shear deformation resistance of H-ACRL and L-ACRL was significantly higher than that of the base asphalt. The addition of modifiers, surfactants, diluents, and reinforcing agent increased the elastic part and enhanced the deformation resistance of the base asphalt system. The G* and G*/sinδ values of H-ACRL were greater than those of L-ACRL at the same temperature, indicating that the deformation resistance of H-ACRL was better than that of L-ACRL.

Figure 5b shows that δ increased with temperature, which was related to the transition of asphalt from a highly-elastic state to a viscous-flow state, as mentioned above. At the same temperature, both types of ACRL showed δ values significantly lower than that of the base asphalt, indicating that the elastic recovery ability of the two ACRLs was significantly better than that of the base asphalt. The addition of modifiers, surfactants, diluents, and reinforcing agent endowed the asphalt with more elastic components, which improved its deformation recovery ability at high temperatures. Additionally, the δ value of L-ACRL was less than H-ACRL at the same temperature, indicating that the contribution of elastic components in H-ACRL was higher, and its deformation recovery was better.

Figure 6a–c shows that after short-term aging, the complex shear modulus G* and rutting factor G*/sinδ increased, while the phase angle δ significantly decreased. These changes indicate that the high-temperature performance of the asphalt was significantly improved, mainly because the gel of polyphosphoric acid increases the content of green and medium-hard components. The gel effect of polyphosphoric acid on asphalt is not affected by the degree of asphalt aging. Under short-term aging, polyphosphoric acid-modified asphalt has a higher content of hard components. The increase in the content of hard components in asphalt enhances the elasticity of asphalt and improves high-temperature performance [24–26].

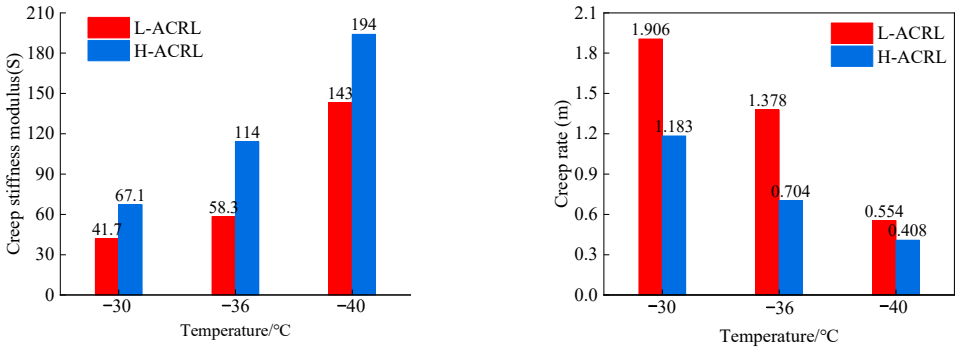


(**a**) Complex shear modulus (G*)/kPa (**b**) Phase angle (δ)/ (°) (**c**) Rutting factor (G*/sinδ)

Figure 6. Temperature-scanning test results after TFOT.

3.3.2. Low-Temperature Rheological Properties

The low-temperature rheological properties of the asphalt materials were characterized by their creep stiffness modulus (S) and creep rate (m), obtained from BBR tests [27]. The H-ACRL, L-ACRL, and base asphalt were tested using a bending beam rheometer, and the results are shown in Figure 7.



(**a**) Creep stiffness modulus (S) (**b**) Creep rate (m)

Figure 7. Rheological test results of curved beams.

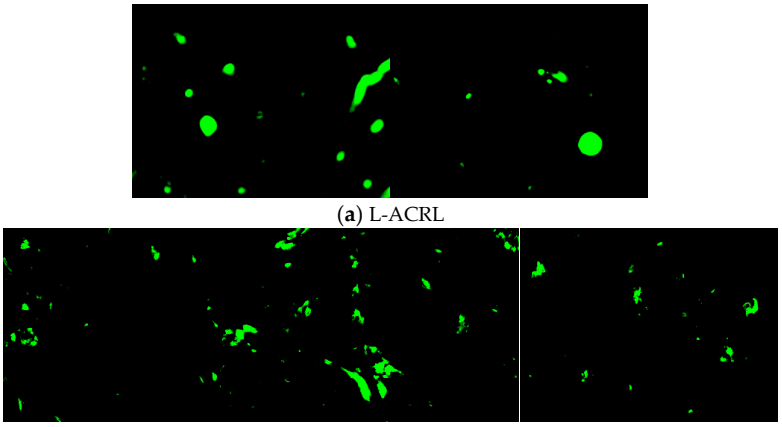
For asphalt, the smaller the S value, the higher the m value, indicating improved low-temperature performance. As shown in Figure 7a, the S value of each asphalt sample gradually increased upon decreasing the temperature. At the same temperature, the S value of low-temperature and high-temperature cold replenishment fluids significantly decreased compared with those of the base asphalt. L-ACRL had a smaller S value than H-ACRL, indicating better low-temperature flexibility, which is consistent with the low-temperature ductility tests. Figure 7b shows that the m value of each asphalt material changed with the temperature, following exactly the opposite trend of the S value. At the same temperature, the m value of L-ACRL was greater than that of H-ACRL, indicating that L-ACRL had better stress relaxation ability and greater elastic recovery in low-temperature environments. In addition, the specifications stipulate that asphalt materials should have values of $S \leq 300$ MPa and $m \geq 0.3$. As shown in Figure 7, both ACRLs meet these specifications at −40 °C, indicating that adding modifiers, surfactants, diluents, and reinforcing agent improved the low-temperature flexibility of asphalt and reduced low-temperature cracking.

L-ACRL had a better effect on improving the low-temperature performance of asphalt than H-ACRL.

3.4. Microscopic Mechanism Analysis of PPA/SBS/SBR Composite-Modified Asphalt Cold Replenishment Liquid

3.4.1. Fluorescence Microscopy

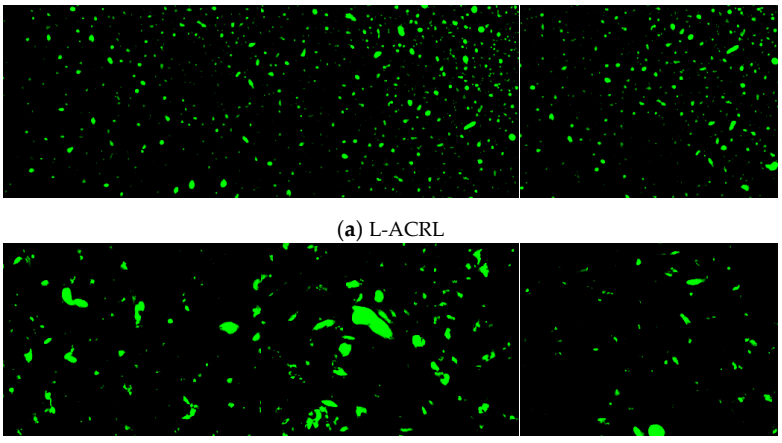
The compatibility between asphalt and modifiers in PPA/SBS/SBR composite-modified asphalt significantly impacts the performance of the blend. H-ACRL and L-ACRL TFOT were used to study the effect of additives such as PPA/SBS/SBR on the microstructure distribution of ACRL. The fluorescence microscopy images before and after adding ACRL and TFOT are shown in Figures 8 and 9. The bright-green fluorescent dots in the figure represent the PPA/SBS/SBR modifier particles dispersed in the asphalt, while the dark parts represent asphalt. The observation results before the aging of the asphalt cold replacement solution are shown in Figure 8. There were more polymer particles dispersed in the asphalt, and the polymer particles in the asphalt were larger and had a clear interface with the asphalt, indicating that the compatibility between adding PPA/SBS/SBR modifier and asphalt was still poor [28]. The addition of polyphosphate did not improve the compatibility between the polymer and asphalt. The observation results after short-term aging of the asphalt cold replacement solution are shown in Figure 9. Compared with the observation before aging, the particle size of polymer particles in asphalt significantly decreased and the number increased, indicating that the polymer underwent significant degradation during the aging process, and the compatibility between the polymer and asphalt was improved [29,30].



(**a**) L-ACRL

(**b**) H-ACRL

Figure 8. Fluorescence microscope image before TFOT.



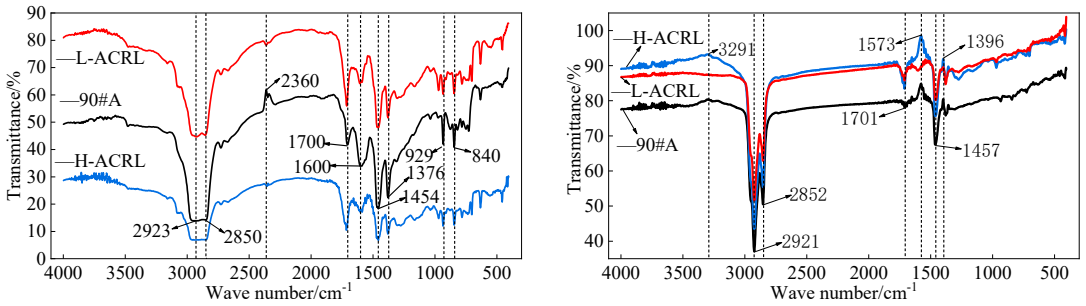
(**a**) L-ACRL

(**b**) H-ACRL

Figure 9. Fluorescence microscope image after TFOT.

3.4.2. Fourier-Transform Infrared Spectroscopy

FTIR spectroscopy was used to determine the functional groups and their changes in various materials, study the chemical reactions occurring during the modification process, and explore the modification mechanism. The FTIR spectra of the materials are shown in Figure 10 [31]. Base asphalt, H-ACRL, and L-ACRL were taken as the research objects before and after TFOT. As shown by the FTIR spectra of different asphalt samples in Figure 10, the FTIR spectra of the two ACRLs were very similar to those of the base asphalt. After TFOT, there were no new absorption peaks generated, and some absorption peaks were only slightly different in intensity [32]. For example, the absorption peaks at 2923 cm^{-1} and 2850 cm^{-1} were caused by $–CH_2$ antisymmetric and symmetric stretching vibrations. There were weaker absorption peaks at 1600 cm^{-1} and 1573 cm^{-1}, which were caused by the stretching vibration of the C=C aromatic ring. The absorption peaks at 1454 cm^{-1} and 1457 cm^{-1} were caused by $–CH_2$ bending vibrations. The peaks in the wavenumber range of 926–840 cm^{-1} were due to the substitution pattern of the benzene ring of asphalt, and several weak absorption peaks appearing in this range were due to C-H vibrations on the benzene ring [33].



(**a**) before TFOT (**b**) after TFOT

Figure 10. FTIR images before and after TFOT.

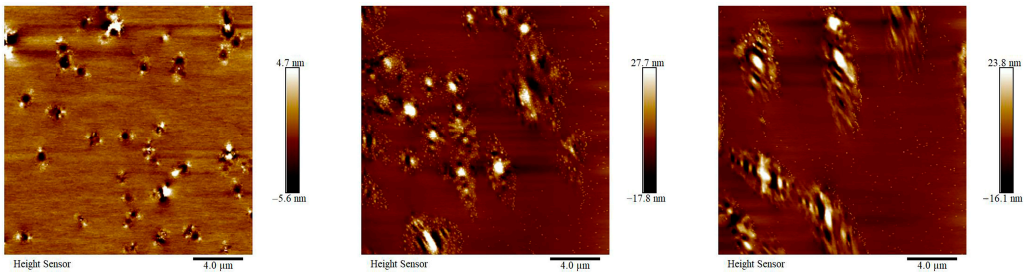
In summary, there were no new absorption peaks for H-ACRL and L-ACRL compared with the spectrum of base asphalt. The process of preparing asphalt cold replenishment liquid by adding modifiers, surfactants, diluents, and reinforcing agent is only a physical modification.

3.4.3. Atomic Force Microscopy (AFM)

AFM can be used to observe the surface morphology of samples to study the microstructure of asphalt materials [34,35]. In addition to observing the microstructure, it can also be used to obtain micro-mechanical information such as the modulus, viscosity, and sample deformation [36,37]. Tapping mode has a higher resolution than contact mode, while non-contact mode causes minimal damage to the sample. Therefore, this article used tapping mode. The 3D AFM images of base asphalt, H-ACRL, and L-ACRL are shown in Figure 11, in which obvious peak-like structures can be observed in all three types of asphalt. These peaks were the three-dimensional representation of the honeycomb structure, whose generation was the result of interactions between paraffin crystals in asphalt and other components [38].

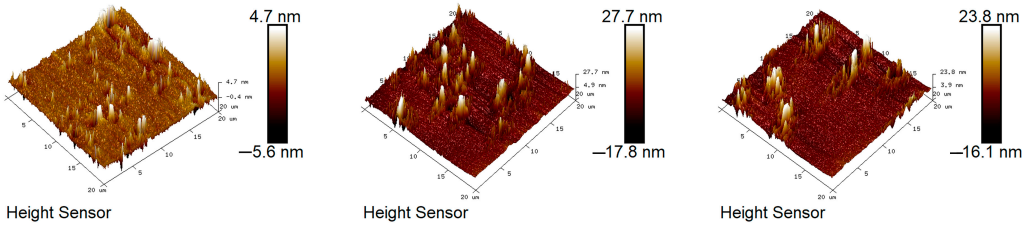
Figure 11 shows the AFM phase diagram and three-dimensional morphology of base asphalt, H-ACRL, and L-ACRL. The three-dimensional morphology map shows wrinkles and undulations on the surfaces of all three types of asphalt. As shown in Figure 12a, the surface of the base asphalt was composed of a honeycomb structure and a plain area, with folds and undulations ranging from −5.6 nm to 4.7 nm. In Figure 12b,c, the surface structures of H-ACRL and L-ACRL were significantly more complex than those of base asphalt, with distinct honeycomb-shaped areas and plain areas. The folded area corresponded to the honeycomb-shaped structure. The surface wrinkling degree of H-ACRL was larger, more than five times that of the base asphalt, reaching −16.1 nm to

27.7 nm. No chemical reactions occurred within the asphalt system, and the original molecular structure of the base asphalt was not altered. In addition, the surface roughness of H-ACRL and L-ACRL was significantly higher than that of base asphalt, and the contact area between the asphalt and the aggregate increased, which improved adhesion [39].



(**a**) Base asphalt (**b**) H-ACRL (**c**) L-ACRL

Figure 11. AFM phase diagram.



(**a**) Base asphalt (**b**) H-ACRL (**c**) L-ACRL

Figure 12. AFM 3D Morphology diagram.

4. Conclusions

The purpose of this study was to analyze the rheological properties and microscopic mechanisms of asphalt cold replacement solution after adding modifiers, surfactants, diluents, and reinforcing agent, using base asphalt as a reference group. The purpose of composite modification of base asphalt is to improve its performance indicators and provide a reference for the next step of CMA improvement. Based on the research results, we can draw the following conclusions:

(1) A total of 25 sets of experiments were conducted using a combination of 6 factors and 5 levels in an orthogonal experimental plan. The orthogonal experiments were processed using factor-level and range analysis methods to determine the optimal mixing ratio of two types of ACRLs. The optimal dosage of H-ACRL is (SBS/SBR/erucamide/polyphosphate/diesel/acrylic ester) (5%/3%/0.9%/1.2%/15%/5%). The optimal dosage of L-ACRL is (SBS/SBR/erucamide/polyphosphate/diesel/acrylic ester) (4%/4%/1.5%/0.9%/18%/7%).

(2) After adding modifiers, surfactants, diluents, and reinforcing agent to the base asphalt, the penetration, softening point, and ductility of the asphalt increased by more than 25%.

(3) Through DSR and BBR experiments, research has shown that the shear deformation resistance and low-temperature flexibility of H-ACRL and L-ACRL were improved compared to the base asphalt. Compared to base asphalt, H-ACRL and L-ACRL had superior high- and low-temperature performance.

(4) Through fluorescence microscopy and FTIR experiments, this research has shown that the compatibility between the addition of modifiers, surfactants, diluents, and reinforcing agent and asphalt was still poor, and the addition of PPA did not improve the compatibility between the polymer and asphalt. Comparing before and after aging, it was found that the particle size of polymer particles in asphalt significantly decreased and the number increased, indicating significant degradation of the polymer during the aging process and improved compatibility between the polymer and asphalt.

(5) This research has shown that there was no chemical reaction between the addition of modifiers, surfactants, diluents, and reinforcing agent and asphalt, and the original molecular structure of the base asphalt was not changed. The surface roughness of H-ACRL and L-ACRL was significantly higher than that of base asphalt, and the contact area between asphalt and aggregate increased, resulting in improved adhesion.

Author Contributions: Methodology, Z.Y.; Formal analysis, X.B.; Investigation, Y.X.; Resources, X.L.; Writing–original draft, L.M.; Writing–review & editing, Y.Z.; Supervision, Z.Z.; Funding acquisition, S.L. All authors have read and agreed to the published version of the manuscript.

Funding: This research was funded by Natural Science Foundation Project of Xinjiang Uygur Autonomous Region in 2023. And All China Federation of Trade Unions Employee Innovation Subsidy Fund Project.

Institutional Review Board Statement: Not applicable.

Informed Consent Statement: Not applicable.

Data Availability Statement: Not applicable.

Conflicts of Interest: The authors declare no conflict of interest.

References

1. Dong, Q.; Gao, J.L.; Chen, X.Q.; Wang, X. Development of a Turpentine Cutback Asphalt Mixture for Porous Pavement Pothole Repair. *J. Mater. Civ. Eng.* **2020**, *32*, 05020001. [CrossRef]
2. Xu, W.; Shah, Y.I.; Luan, D.X.; Tian, S.B. Evaluation of Moisture Damage of Cold Patch Asphalt Using the Surface Free Energy Method. *Arab. J. Sci. Eng.* **2021**, *46*, 11267–11277. [CrossRef]
3. Hasanuzzaman, M.; Hashemian, L.; Bayat, A. Laboratory Investigations of Cold Mix Asphalt for Cold Region Applications. *J. Test. Eval.* **2018**, *46*, 88–98. [CrossRef]
4. Fedrigo, W.; Nunez, W.P.; Fernandes, D.P.; Malabarba, L.M.; Ceratti, J.A.P.; Brito, L.A.T. Effects of RAP residual asphalt binder type, content and ageing on the mechanical behaviour of cold recycled cement-treated mixtures. *Road Mater. Pavement Des.* **2021**, *22*, 1389–1406. [CrossRef]
5. Pei, Z.S.; Yi, J.Y.; Fan, L.; Yu, W.; Hai, B.E.; Feng, D.C. Analysis of the trend in evolution of multilevel mechanical properties of solvent-based cold mixed liquid asphalt and mixture. *Constr. Build. Mater.* **2022**, *335*, 127476. [CrossRef]
6. Hafezzadeh, R.; Autelitano, F.; Giuliani, F. Asphalt-based cold patches for repairing road potholes—An overview. *Constr. Build. Mater.* **2021**, *306*, 124870. [CrossRef]
7. Xiao, R.; Polaczyk, P.; Huang, B.S. Measuring moisture damage of asphalt mixtures: The development of a new modified boiling test based on color image processing. *Measurement* **2022**, *190*, 110699. [CrossRef]
8. Ryms, M.; Denda, H.; Jaskula, P. Thermal stabilization and permanent deformation resistance of LWA/PCM-modified asphalt road surfaces. *Constr. Build. Mater.* **2017**, *142*, 328–341. [CrossRef]
9. Bazmara, B.; Tahersima, M.; Behravan, A. RETRACTED: Influence of thermoplastic polyurethane and synthesized polyurethane additive in performance of asphalt pavements (Retracted article. See vol. 380, 2023). *Constr. Build. Mater.* **2018**, *166*, 1–11. [CrossRef]
10. Xu, L.; Li, X.R.; Zong, Q.D.; Xiao, F.P. Chemical, morphological and rheological investigations of SBR/SBS modified asphalt emulsions with waterborne acrylate and polyurethane. *Constr. Build. Mater.* **2021**, *272*, 121972. [CrossRef]
11. Abd El-Rahman, A.M.M.; El-Shafie, M.; Abo-Shanab, Z.L.; El-Kholy, S.A. Modifying asphalt emulsion with different types of polymers for surface treatment applications. *Pet. Sci. Technol.* **2017**, *35*, 1473–1480. [CrossRef]
12. Wang, X.Y.; Huang, Y.K.; Geng, L.T.; Li, M.L.; Han, H.C.; Li, K.; Xu, Q.; Ding, Y.; Zhang, T. Multiscale performance of composite modified cold patch asphalt mixture for pothole repair. *Constr. Build. Mater.* **2023**, *371*, 130729. [CrossRef]
13. Raza, Z.A.; Riaz, S.; Banat, I.M. Polyhydroxyalkanoates: Properties and chemical modification approaches for their functionalization. *Biotechnol. Prog.* **2018**, *34*, 29–41. [CrossRef] [PubMed]
14. Riaz, S.; Park, S.J. A comparative study on nanoinclusion effect of MoS2 nanosheets and MoS2 quantum dots on fracture toughness and interfacial properties of epoxy composites. *Compos. Part A Appl. Sci. Manuf.* **2021**, *146*, 106419. [CrossRef]
15. Raza, Z.A.; ur Rehman, M.S.; Riaz, S. Zinc sulfide mediation of poly (hydroxybutyrate)/poly (lactic acid) nanocomposite film for potential UV protection applications. *Int. J. Biol. Macromol.* **2022**, *222*, 2072–2082. [CrossRef] [PubMed]
16. Yang, J. Research on the high and low temperature performance and anti-aging ability of polyphosphoric acid/SBR composite modified asphalt. *J. China Foreign Highw.* **2019**, *39*, 249–254. (In Chinese)
17. Wei, J.; Shi, S.; Zhou, Y.; Chen, Z.; Yu, F.; Peng, Z.; Duan, X. Research on Performance of SBS-PPA and SBR-PPA Compound Modified Asphalts. *Materials* **2022**, *15*, 2112. [CrossRef]
18. Eaton, P.E.; Carlson, G.R.; Lee, J.T. Phosphorus pentoxide-methanesulfonic acid. Convenient alternative to polyphosphoric acid. *J. Org. Chem.* **1973**, *38*, 4071–4073. [CrossRef]

19. Vekariya, R.H.; Prajapati, N.P.; Patel, H.D. Silica-supported polyphosphoric acid (PPA-SiO2): An efficient and reusable heterogeneous catalyst for ecofriendly organic synthesis. *Synth. Commun.* **2016**, *46*, 197–219. [CrossRef]
20. *JTG E20-2011*; Test Specification for Asphalt and Asphalt Mixtures in Highway Engineering. People's Communications Press: Beijing, China, 2011. (In Chinese)
21. *JT/T 972-2015*; Asphalt Pavement Pit Cold Repair Finished Material. People's Communications Press: Beijing, China, 2015. (In Chinese)
22. Walubita, L.F.; Mahmoud, E.; Fuentes, L.; Prakoso, A.; Lee, S.I.; Souliman, M.; Komba, J.J. Correlating the asphalt-binder high-temperature properties (DSR) to HMA permanent deformation (RLPD) and field rutting: A laboratory-field study. *Constr. Build. Mater.* **2020**, *262*, 120761. [CrossRef]
23. Guo, Y.M.; Ni, F.J. Dynamic viscoelastic properties of modified asphalt and mixtures based on DSR. *J. Southeast Univ. (Nat. Sci. Ed.)* **2014**, *44*, 386–390. (In Chinese)
24. Zhang, F.; Yu, J.; Wu, S. Effect of ageing on rheological properties of storage-stable SBS/sulfur-modified asphalts. *J. Hazard. Mater.* **2010**, *182*, 507–517. [CrossRef]
25. Zhang, F.; Yu, J.; Wu, S. Influence of ageing on rheology of SBR/sulfur-modified asphalts. *Polym. Eng. Sci.* **2011**, *52*, 71–79. [CrossRef]
26. Zhang, F. *Study on the Effect of Polyphosphate and Sulfur on the Aging Performance of Polymer Modified Asphalt*; Wuhan University of Technology: Wuhan, China, 2011. (In Chinese)
27. Xia, P.Y.; Hu, L.Q.; Yan, J.; Wang, S.K.; Yang, Z. Low-temperature performance evaluation indices of high-viscosity modified asphalt. *China Sci.* **2020**, *15*, 1417–1421. (In Chinese)
28. Sengoz, B.; Topal, A.; Isikyakar, G. Morphology and image analysis of polymer modified bitumens. *Constr. Build. Mater.* **2009**, *23*, 1986–1992. [CrossRef]
29. Virginie, M.; Jérôme, L.; Françoise, D.; Jean-Pascal, P.; Laurence, L. Infrared microscopy investigation of oxidation and phase evolution in bitumen modified with polymers. *Fuel* **2008**, *87*, 1270–1280.
30. Jérome, L.; Francoise, D.; Jean-Pascal, P.; Virginie, M.; Jacky, K. Direct and continuous methodological approach to study the ageing of fossil organic material by infrared microspectrometry imaging: Application to polymer modified bitumen. *Anal. Chim. Acta* **2011**, *444*, 241–250.
31. Dong, G. Performance and Mechanism of Asphalt Modified with Polyphosphoric Acid and Polyphosphoric Acid/Polymer. Ph.D. Thesis, Chang'an University, Xi'an, China, 2019. (In Chinese).
32. Chen, L.Q.; Zhang, Z.P.; Huang, T.; Ban, X.Y.; Liu, H. Preparation and application properties of high-viscosity modifier HVM-TSR. *China Sci.* **2022**, *17*, 1408–1414. (In Chinese)
33. Guo, N.S.; Yu, C.H.; Wang, L.; Jin, X.; Wen, Y.K. Rheological and Microscopic Properties of PR.M/Crumb Rubber Composite Modified Asphalt. *Mater. Rep.* **2021**, *35*, 10080–10087. (In Chinese)
34. Navarro, F.J.; Partal, P.; Garcia-Morales, M.; Martinez-Boza, F.J.; Gallegos, C. Bitumen modification with a low-molecular-weight reactive isocyanate-terminated polymer. *Fuel* **2007**, *86*, 2291–2299. [CrossRef]
35. Ortega, F.J.; Roman, C.; Navarro, F.J.; Garcia-Morales, M.; McNally, T. Physico-chemistry control of the linear viscoelastic behaviour of bitumen/montmorillonite/MDI ternary composites: Effect of the modification sequence. *Fuel Process. Technol.* **2016**, *143*, 195–203. [CrossRef]
36. Das, P.K.; Baaj, H.; Tighe, S.; Kringos, N. Atomic force microscopy to investigate asphalt binders: A state-of-the-art review. *Road Mater. Pavement Des.* **2016**, *17*, 693–718. [CrossRef]
37. Wang, B.H.; Chen, J.L.; Zhang, B. Application of Atomic Force Microscopy in Polymer Characterization. *Acta Polym. Sin.* **2021**, *52*, 1406–1420.
38. Polacco, G.; Filippi, S.; Merusi, F.; Stastna, G. A review of the fundamentals of polymer-modified asphalts: Asphalt/polymer interactions and principles of compatibility. *Adv. Colloid Interface Sci.* **2015**, *224*, 72–112. [CrossRef] [PubMed]
39. Dai, Z.; Zhu, H.; Shen, J.N. Application of Atomic Force Microscopy (AFM) on Asphalt Surface Microstructure. *East China Highw.* **2017**, *6*, 94–98. (In Chinese)

Disclaimer/Publisher's Note: The statements, opinions and data contained in all publications are solely those of the individual author(s) and contributor(s) and not of MDPI and/or the editor(s). MDPI and/or the editor(s) disclaim responsibility for any injury to people or property resulting from any ideas, methods, instructions or products referred to in the content.